SYSTEMATIC ANALYSIS OF THE QUASAR PROPERTIES AND VARIABILITY OF EXTREMELY-HIGH VELOCITY OUTFLOW QUASARS IN THE SLOAN DIGITAL SKY SURVEY

Easton Pierce, Alex Vong, Abby Wang, Cora DeFrancisco, Anish Rijal, Tzitzi Romo Pérez, Mikel Charles, Wendy García Naranjo, Rachel Fulda, Veronica Powell, Lorena Sanabria

ABSTRACT: Active Galactic Nuclei host a super massive black hole surrounded by in-falling gas in the form of an accretion disk. The most luminous of them, called quasars, regularly present outflowing winds, observed as absorption in their spectra. These winds may play a large role in galactic and black hole evolution. Extremely High Velocity Outflows (EHVOs), which are outflows with speeds of > 10% the speed of light, are the least understood type of these outflows.

We present the preliminary results on the first systematic study on EHVO quasar properties and variability of these extreme outflows in the 16th data release (DR16) of the Sloan Digital Sky Survey. Of the 98 quasars with EHVOs discovered in the DR16, 51 cases were inspected for variability because they had multiple observations in other data releases. We find that 47% of them show variability. Velocity and depth changes were both observed via the shifting of our absorption and the disappearance and appearance of EHVOs respectively. Of the 98 quasars with EHVOs, we have values of physical properties, such as bolometric luminosity, black hole mass and Eddington ratio, for 69 cases. We find that quasars with EHVOs exhibit larger values of their bolometric luminosity and Eddington ratio when compared to Broad Absorption Line Quasi-Stellar Objects (BALQSOs) and non-BAL parent sample quasars, while the black hole mass parameter does not show significant differences.

Definitions:

- *BALQSO: Broad Absorption Line Quasi-Stellar Object. A quasar that exhibits a Broad Absorption Line (BAL) in its spectrum.*
- *BAL: Broad Absorption Line. Caused by a gas cloud around the black hole absorbing a large range of wavelengths and is identified by an absorption trough or dip that is at least 2000 km s^{-1} in width.*
- *Continuum: The distribution of energy at different wavelengths of light. Quasars follow a power law continuum, where the intensity of light instead follows a power law which skews higher intensity towards the shorter wavelengths. The continuum is used as a baseline to measure absorption and emission, i.e. dips below the continuum are measured as absorption and peaks above are measured as emission.*
- *EHVO: Extremely High Velocity Outflow, gas outflowing from around the quasar at more than 10% the speed of light. These outflows can be identified by absorption of CIV in their spectrum; this CIV absorption shows up as a trough in the continuum shifted at least 10% the speed of light from the CVI emission line.*
- *Flux: The amount of light energy our instruments receive per second.*
- *Parent sample: A larger group or sample from which a smaller group or sample is drawn. A parent sample of BALQSOs would be quasars, as all BALQSOs are quasars but not all quasars are BALQSOs. BALQSOs are a subset of quasars.*
- *Quasar: Extremely luminous objects caused by the friction of gas falling into a black hole.*

1. Introduction

Quasi-stellar radio sources, or "quasars" as coined by astrophysicist Hong-Yee-Chiu, were named as such because these mysterious objects look to us like stars but show very different spectra and sometimes emitted radio waves. Located at the centers of galaxies, quasars are some of the most luminous objects found in the universe. The luminosity of an object is measured by how much electromagnetic energy (what we commonly understand as light) is emitted over time. For instance, the luminosity of the sun, also known as solar luminosity, has a value of 3.846×10^{26} watts (or 3.846×10^{33} ergs per second). In comparison, the luminosity of an average quasar is about 10^{40} watts, roughly $2.6 * 10^{13}$ times that of the sun (Ryden 2016). In fact, quasars are a subtype of regions at the centers of galaxies that have higher-than-normal luminosities, known as Active Galactic Nuclei (AGN). Today, it is generally believed that the high luminosities of quasars, and AGNs in general, are powered by supermassive black holes (SMBH).

However, a black hole does not emit observable light since not even light can escape a black hole's gravitational pull. Then, how do we observe quasars? With mass that is millions or billions of times the mass of the Sun, a super massive black hole creates an enormous gravitational pull that powers the quasar by attracting matter and forming an accretion disk (Dunbar 2007). The emissions we observe are from these environments surrounding the black hole..

A subset of BALQSOs, known as Extremely High Velocity Outflows (EHVOs), present winds moving faster than 10% the speed of light. Figure 1 shows an example of the spectrum of a quasar with an EHVO. These EHVOs are still poorly understood, but they play a role in galaxy formation, due to their enormous energies that are able to disperse large amounts of gas and disrupt the star formation processes in the galaxy around them (Di Matteo et al. 2005). It is also hypothesized that these EHVOs help accelerate the mass growth rate of supermassive black holes. This is because these outflows "steal" angular momentum from the accretion disk, increasing the efficiency of in-fall mass rate (Emmering et al. 1992; Konigl & Kartje 1994).

The spectrum of a celestial body is the result of the light as it passes through a prism or a spectrograph and the light is dispersed in its

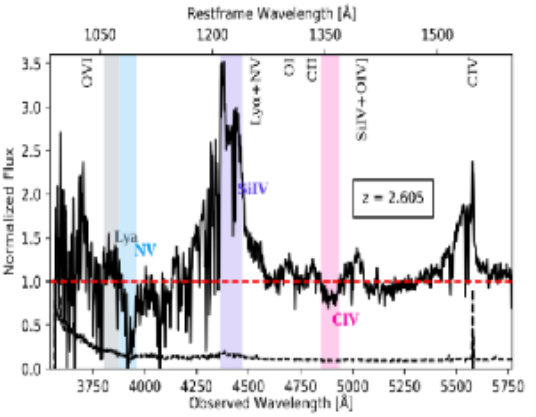

Figure 1: Example spectrum of an EHVO quasar at redshift z = 2.605 displaying flux (solid) and error (dashed). The EHVO is identified by the CIV absorption (highlighted in pink) centered at approximately 1370 Å in rest-frame wavelength (shown at the top). Absorption features caused by other ions in the same outflow and similar speeds are also outlined in their respective colors: Ly-α (gray), NV (cyan), SiIV (blue). A red-dashed line is graphed at the normalized flux of 1, representing where the flux fits the continuum. Both x-axes are measurements of wavelength, one at the rest-frame (from 1000-1600 Å) of the quasar (top) and the other as we observed it (from approximately 3500-5800 Å - bottom), both in units of angstroms Å (10-10 meters). The y-axis is a unitless normalized value of flux. Locations of emission lines are also highlighted along the top of the graph for CIV, SiIV+OIV, CII, OI, and Ly-α+NV.

wavelengths. It provides information about the chemical composition of the object thanks to the fact that each element in the periodic table has specific energy levels that the electrons can inhabit (Knight 2016). These levels are unique to each atom. When an electron drops in energy level, it emits the difference in the form of light. These energies are inversely proportional to the wavelength of light emitted. These emissions create a signature that is observable in the quasar's spectrum as an emission line. Electrons are also able to jump up in energy level by absorbing light, which shows up as an absorption trough or dip in the spectrum. The study of these emissions and absorptions allows for the understanding of the nature of the elements present in the environment of the quasar, such as carbon, hydrogen, silicon, etc.

Due to the expansion of the universe, the quasar spectrum is shifted towards longer (redder) wavelengths. The magnitude of this redshifting is given a value "z". Astronomers always give the prefix "rest-frame" when talking about properties from the perspective of the object. Thus, the wavelength of light as it was emitted, before being redshifted, is called the rest-frame wavelength. This z- value is defined as $(\lambda_{observed} - \lambda_{rest\text{-}frame})/\lambda_{rest\text{-}frame}$. The EHVOs in this paper ranged from z = 1.914 to 4.479. In Figure 1 we show an example of a quasar at redshift z = 2.605, the rest-frame wavelength ($\lambda_{rest\text{-}frame}$) is indicated at the top of the spectrum and what we observe on Earth at the bottom ($\lambda_{observed}$).

This paper is a research-in-progress update covering two projects both analyzing different features of the 98 new EHVO cases identified in Rodríguez Hidalgo et al. (in prep). The variability project aims to identify how EHVOs change over time, and how often this change occurs. The quasar properties project aims to identify whether EHVOs have distinct physical properties when compared to BALQSOs and the parent sample, which also includes non-BALQSOs.

In this paper we describe the data we use in Section 2, analysis and discussion of variability in Section 3, analysis and discussion of quasar properties showing EHVOs in Section 4, and Section 5 is a summary.

2. Data

All of the data presented in this paper originates from the Sloan Digital Sky Survey (SDSS), whose observations were taken with the 2.5m telescope located at Apache Point Observatory in New Mexico. This archival data is regularly released in batches called Data Releases (DR), the most recent of which DR16 was made public on Dec 9th, 2019. Each quasar observation is identifiable by three numbers: plate, MJD, and fiber. To observe multiple objects simultaneously, the 2.5m telescope utilizes specially manufactured aluminum plates. These plates contain hundreds of holes each including an individual optical fiber, whose location corresponds to where in the focal plane of the telescope the objects are observed. A Modified Julian Date (MJD) is a convention mainly used in astronomy that counts the number of days since midnight on November 17th, 1858. This makes tracking large date changes easier, as the difference in MJD between two dates is simply the number of days between them. Previously 40 EHVOs quasars were identified in DR9 (Rodríguez Hidalgo et al. 2020), with an additional 98 having been confirmed from DR16 (Rodríguez Hidalgo et al. in prep). This current study focuses on the latest findings.

Of the 98 cases, we find that 51 have observations at multiple epochs (observations at different times) which are discussed in Section 3. When measuring quasar properties, we have data for 69 of these cases, which are discussed in Section 4.

3. Analysis and Discussion of Results of Variability of Extremely High Velocity Outflows.

3.1 Previous studies in Variability.

EHVOs, like BALQSOs, sometimes exhibit variability in their absorption profiles (e.g., Rodríguez Hidalgo 2011; Rogerson et al. 2016). This manifests as depth changes in BAL troughs, or speed changes between observations. Depth changes, i.e., absorption strength changes, can be observed ultimately as appearance or complete disappearance of absorption altogether. If the speed of the outflow increases then the trough would shift to a shorter wavelength, and vice versa for a speed decrease.

Previous studies on variability in EHVOs have focused on specific quasars, as in the case of J023011.28+005913.6 (Rogerson et al. 2016) or have been more broadly studying the slower BALQSOs. This is the first systematic study of variability in EHVOs. The causes of variability in EHVOs is currently unknown but, as EHVOs are a subset of BALQSOs, the mechanism behind their variability might be related. There are two prevailing theories as to the origin of observed variation in BALQSOs. The first assumes that all the difference in absorption features observed can be explained purely by the transverse motion of gas clouds in or around the accretion disk, blocking our sightline to the quasar (Boroson et al. 1991). The underlying absorption parameters of the gas are unchanged (energies, ionization, etc.) and any new absorption features are caused by the light's absorption by this new cloud. The second assumes that the absorption changes are caused by actual changes in the ionization parameters of the outflow gas (Barlow et al. 1992). This implies a dimming or brightening of the continuum flux (decrease and increase in energy). This difference in energies results in different levels of ionization in the present atoms, causing different absorption features. For example: if more ionizing radiation is present, instead of finding CIV (carbon where 3 electrons have been removed by the incident light) we might find CV (carbon where 4 electrons have been removed). If all of the absorption features present at different speeds, and therefore likely at different distances from the source, change in unison, known as coordinated variability, then we most likely have a change in the underlying ionization parameters, as a gas cloud passing between us and the quasar cannot account for absorption changes across the entire continuum.

Studying variability can grant us greater insight into the nature of the outflow environment.We can use variability to place a constraint on the density and distance of the absorbing gas from the black hole (Hamann et al. 1995). If we assume we are in an ionization equilibrium, i.e., the number of gas particles being ionized per second is the same as the number of gas particles recombining per second, then the equation can

$$n \approx \frac{1}{\alpha * t_{recombination}}$$

be used to find the density (n), where α is the ionization parameter (a constant specific to each ion), and $t_{recombination}$ is the recombination time. If the time between observations in the rest-frame is the upper limit for $t_{recombination}$, then a lower limit can be placed on the density of the gas. Ifthe bolometric luminosity L_{bol} (see Section 4) is also known, then the distance between the black hole and the absorbing gas (R) can be constrained using where U is the ionization.

$$U \approx \frac{L_{bol}}{n * R^2}$$

If the cause of variability is assumed to be the transverse motion of a gas cloud, and we assume that the speed of this gas cloud has reached the speed of our outflow, then the lower limit on the distance of the cloud can also be constrained via Kepler's equations of orbital motion.

3.2 Our Results.

As mentioned previously, 51 EHVOs had observations at different epochs. For each case, two or more epochs were graphed against each other to compare their absorption profiles. These graphs were plotted between the rest-frame wavelengths of 1225-1600 Å, as this region contains our EHVO CIV absorption whenever present. For our report in progress, these graphs were unnormalized. This normalization process aims to fit the parts without absorption and emission with a power law through the use of an algorithm developed by our team previously (Charles et al. 2022). This normalization algorithm chooses 3 anchor points, each in a region where no absorption or emission features are present. This allows the program to be confident in fitting the power law continuum instead of absorption or emission features. The spectra is then divided by this power law, and the result is the normalization flux. Because normalizing makes the comparison of absorption features easier between the epochs, there is a certain degree of uncertainty in measuring variability in the unnormalized graphs. This paired with poor signal-to-noise ratios in older observations and missing flux data in certain epochs resulted in variability being classified into three groups: confirmed, uncertain, or none. All cases were visually inspected for variability, with measurements to follow in a future report. Time differences between observations varied from those made on the same day and differences of 5573 days in our reference frame. Because these objects experience time slower the further away they are. The rest-frame time between observations is the MJD difference / (z +1), which results in time differences of less than a day and 1772 days, respectively, in the rest-frame of our quasars.

Of the 51 cases, 47% (24/51) were confirmed to exhibit some degree of variability. Our team observed all three manifestations of variability outlined previously. Figure 2 shows the appearance of an EHVO in the quasar J103800.50+582343.0 between MJD 52428 and MJD 56661 ($\Delta t_{rest\text{-}frame}$ = 1143 days) via an increase in CIV absorption (shown in pink) centered at 1360 Å in the rest-frame.

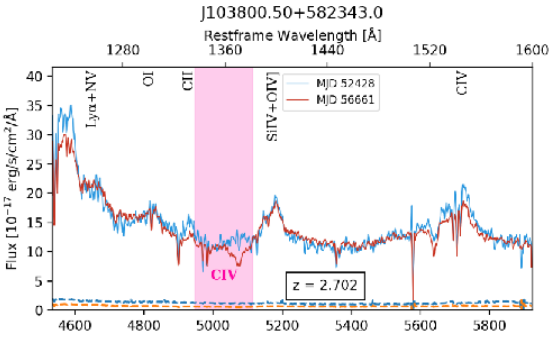

Figure 2: Appearance of an EHVO in J103800.50+5823432.0 with redshift z = 2.702, between the observations MJD 52428 (blue) and MJD 56661 (red) via the emergence of CIV absorption centered around 1360 rest-frame wavelength. As with Figure 1, both x-axes are measurements of wavelength, with different rest-frame and observed limits, from 1225-1600 Å and from approximately 4500-5900 Å respectively. The y-axis is a flux value scaled by the wavelength observed in units of erg/s/cm2/Å. The location of our CIV absorption is outlined in pink. Locations of emission lines are also highlighted along the top of the graph for CIV, SiIV+OIV, CII, OI, and Ly-α+NV.

Figure 3: Disappearance of an EHVO in quasar J004300.26+045718.6 between MJD 55867 (blue) and MJD 58082 (red) with redshift z =2.362. Axes and labels are similar to those in Figure 2.

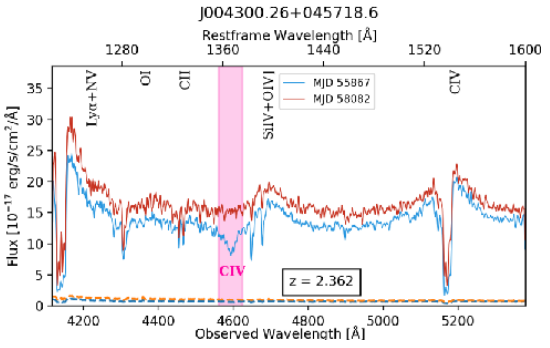

Figure 3 shows the disappearance of an EHVO was observed in quasar J004300.26+045718.6 via the loss of CIV absorption between MJD 55867 and MJD 58082 ($\Delta t_{rest\text{-}frame}$ = 658 days).
Our team also observed speed changes as exemplified in J000022.93-022716.4 (see Figure 4), with a possible outflow acceleration of approximately 5200 km s-1 between MJD 55810 and 57713 ($\Delta t_{rest\text{-}frame}$ = 527 days).

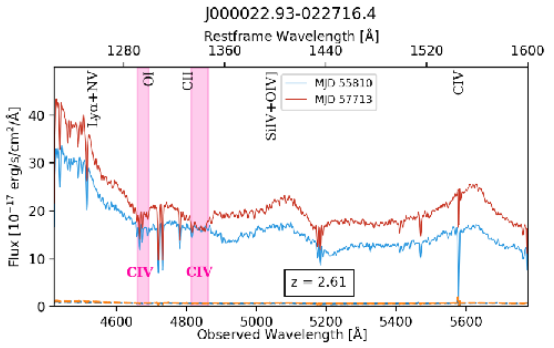

Figure 4: Shifting of CIV absorption from approximately -36500 km s^{-1} to -41747 km s^{-1} suggests potential acceleration of the EHVO in the quasar J000022.93-022716.4 between MJD 55810 (blue) and 57713 (red). Axes and labels are similar to those in Figure 2.

A further 20 out of 51 cases (39%) are likely to show some variability but our results are still uncertain since we will need to normalize the spectrum to classify them appropriately. Our team observed no variability in 7 of the 51 cases (14%).

Our results indicate that EHVOs show more frequent variability than BALs at lower speed. Filiz et al. (2013) showed that approximately 57.9% BALQSOs were found to have CIV variability. Using the potential changes in ionization, shorter recombination times will require larger densities of the gas. Assuming all other parameters are similar, this would imply that EHVOs are at closer distances to the ionizing source than BALQSOs. However, as noted in Section 4.2, EHVO quasars show larger bolometric luminosities than BALQSOs, and therefore this will affect the distances as well, likely mitigating the larger densities.

3.3 Future Work in Variability:

To measure quantitatively how much these absorption profiles have varied and be able to compare them to previous studies in BALQSOs, we are in the process of normalizing our spectra via the method outlined in Charles et al. 2022. Once the spectra are normalized, we will quantify the variability via three values: the equivalent width (EW), which is defined as the width of a rectangle with height from the continuum line to zero containing an equivalent area as the absorption line, the average depth of our absorption troughs, and lastly the changes in velocity.

A region of the spectrum known as the Lyman alpha (Ly-α) forest is of particular interest to our team. This is the region below a rest-frame wavelength of 1216 Å and coincides with the energy required to excite hydrogen to its first excited state. Each time light from the quasar interacts with a hydrogen gas cloud along its journey, part of the spectrum is absorbed by that hydrogen and re-emitted in a random direction. The likelihood of the re-emission direction lining

back up with its original direction is functionally zero, which results in a narrow absorption line, as the light is effectively eliminated from our spectrum. However, as the light encounters different galaxies with different redshift values on its journey toward us, the narrow hydrogen absorption line appears at different wavelength values in the spectrum, resulting in dozens to sometimes hundreds of narrow lines spread across the Ly-α region. This is a larger issue with high redshift objects, as objects further away have significantly more lines obscuring our spectrum.

This region is important to study because we can look for ions that are shifted into that part of the spectrum. This allows for the identification of EHVOs at higher outflow speeds, because as the speed of an outflow increases, the more shifted towards the blue our absorption features are. This tends to push absorption features of high speed EHVOs into the Ly-α forest. Furthermore, CIV absorption on its own still leaves a large uncertainty in the ionization parameters of the quasar, each successive ion we observe absorption in allows us to hone in on a more accurate view of the conditions of the gas in our system.

In the future we will remove the Ly-α lines with code developed previously by our team. The Ly-α code is open-source software designed to filter out Lyman-alpha forest lines from multi-epoch observations of quasars with EHVOs while leaving the underlying absorption intact. Using results from Bosman et al. 2022 we are able to normalize the Lyman-alpha forest region of the quasar's spectra. This normalization technique is tailored for the Ly-α region and thus distinct from the one outlined in Charles et al. 2022. Because the Ly-α absorption caused by the hydrogen gas clouds don't usually vary at the timescales we observe EHVO variability, multi-epoch observations help identify intervening absorption caused by the hydrogen gas versus intrinsic absorption caused by our EHVO. We model individual intervening absorption lines with Gaussian curves. The continuum is modeled with the layering of multiple curves called a cubic spline. Following a simultaneous fit, the absorption features are denoised, revealing a high-precision reconstruction of intrinsic features not attained before. This method allows us to analyze EHVO intrinsic absorption lines that have been shifted into the heavily absorbed Lyman-alpha forest region, including absorption due to multiple ions and their variability.

4. Analysis and Discussion of Results of the Physical Properties of EHVO Quasars.

4.1 Description of Quasar Properties in Our Study

To study the characteristics of the quasars that show EHVOs in their spectra in comparison to other quasars like BALQSOs, we analyze the properties of quasars with EHVOs, such as bolometric luminosity, black hole mass and Eddington ratio, and compare them to those in the populations of BALQSOs and the parent sample.

We do not compute the measurements of these physical properties and instead rely on previously calculated measurements by other research groups. A recent paper (Wu and Shen 2022) includes measurements for these properties in the DR16, however they do not apply Coatman's correction described below. Rankine et al. 2020 has measured these values including this correction but they were not published in the literature; she graciously provided them to us.

The bolometric luminosity (L_{bol}) is the luminosity of an object across all wavelengths. It is often measured relative to the solar luminosity and provides the amount of energy the quasar is releasing. The method of obtaining the bolometric luminosity without having to integrate data at all wavelengths is to use previously tabulated corrections anchored in particular values of the quasar spectrum. This is called bolometric corrections (BC). The values

provided by Rankine include the BC corrections described in Shen et al. (2011): for quasars with z > 1.9, they used the monochromatic luminosity at 1350 A in the rest-frame of the quasar and applied a correction of BC = 3.81.

The black hole mass (M_{bh}) is estimated through measuring the width of the CIV emission line. A standard measurement of the width of emission lines is to compute the full width half maximum (FWHM) which, as the name indicates, is the value of the width calculated at half value of the maximum height of the emission line. If the line is just produced by the movement of gas around a black hole, the width should correlate directly with the mass of the black hole, as more massive black holes will result in faster material around and therefore broader emission lines. However, if the emission includes some material outflowing, the width of the line would be larger and the calculated FWHM would also be artificially large. The result of this is overestimated values of black hole masses. The values from Rankine et al. (2020) have been corrected for this effect using the work of Coatman et al. (2017). However, for cases where this effect is small, the scattering in the measurements does not provide good results and those cases need to be discarded.

As expected, the values provided by Amy Rankine result in more moderate estimates of the black hole mass measurements for EHVO quasars, compared to previous calculations, since the outflow component is not included. Previously in Rodriguez Hidalgo et al. 2020 we used instead black hole mass values provided in Shen et al. 2011 that do not account for the correction, and we observed larger values of black hole mass for quasars with EHVOs relative to the parent population. This makes sense since in Rodriguez Hidalgo and Rankine (2022) our team found that EHVO quasars show larger outflows in the CIV emission line.

The Eddington ratio is defined as a dimensionless ratio of bolometric luminosity over Eddington luminosity (L_{edd}). Eddington luminosity predicts the theoretical maximum luminosity an object can emit. The Eddington ratio is calculated as the ratio between the bolometric luminosity and the black hole mass, both explained above. The Eddington ratio indicates the mass accretion rate of the SMBH in a quasar: a quasar that has a larger Eddington ratio is accreting mass at a faster rate. This clarifies whether EHVO quasars are distinctive when compared to BALQSOs and versus their parent sample.

The challenge in studying DR16 quasars is that Rankine et al. (2020) had only measured the values of quasar physical properties in DR14, so we do not have measurements for all the DR16 EHVO quasars. However, since the data release 16 includes the cases in previous data releases, we do have values for all those quasars that were already in the data release 14. Therefore, our group used a cross-correlation process between the Rankine et al. (2020) DR14 measurements and our quasars. To do so, we developed our own software to match the ` plate, MJD, and fiber numbers between the two data releases. These numbers act like serial numbers, allowing us to trace the same quasars from both DR14 and DR16. As described in section 2, the total number of identified EHVO quasars is 98 cases, and there are 69 cases with physical property information in the DR14. Other quasar groups such as the parent sample and BALQSOs also lose cases through the cross-correlation process. The resulting numbers of each group are then 69 EHVO quasars, 14004 cases of parent sample, and a total of 1866 cases of BALQSOs.

4.2 Our Results.

Figures 5 and 6 show a set of two scatter plots with corresponding histograms of the physical properties of all three quasar groups. Both sets of figures include our EHVO quasars in magenta. Figure 5 includes the parent sample's values in blue, and Figure 6 the BALQSOs in two shades of blue: those BALs with minimum outflow

velocity less than 10,000 km/s are in light blue and those with minimum outflow velocity in between 10,000 km/s and 25,000 km/s region appear in darker blue: Each Figure set includes (a) a comparison between Mbh and the Eddington ratio, while (b) shows L_{bol} versus Eddington ratios.

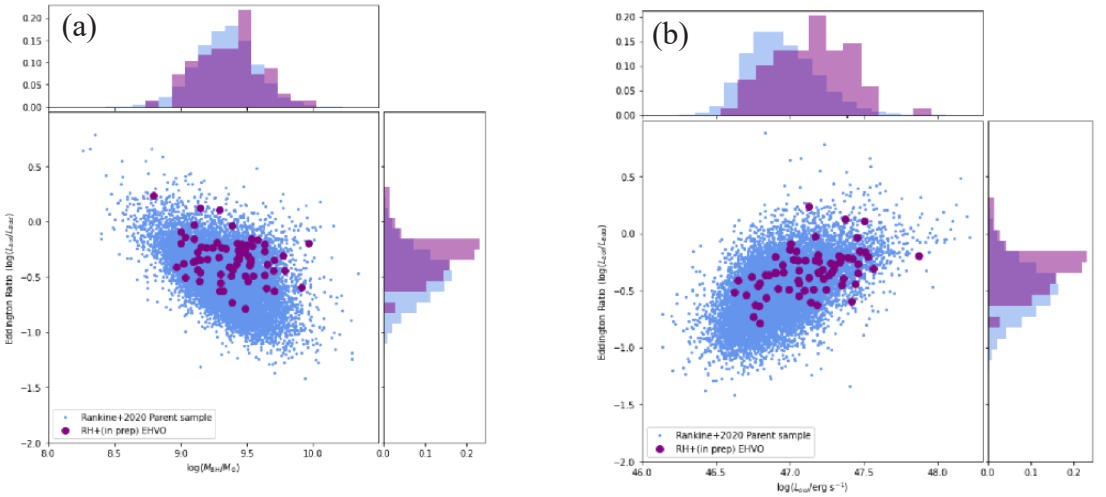

Figure 5. The two plots (a) and (b) include scatter plots at the center and histograms (top and right) of M_{bh} (top), L_{bol} (bottom), and Eddington ratio (right). We plotted the parent sample (blue) vs EHVO quasars (magenta). Scatter plot (upper) shows Eddington ratio against M_{BH} in comparison. The M_{BH} of the EHVOs and parent samples are similar. However, EHVO quasars show larger Eddington ratios than the parent sample. Bottom plot shows Eddington ratio against L_{bol}: we find that the EHVO quasars are more luminous than the quasars in the parent sample.

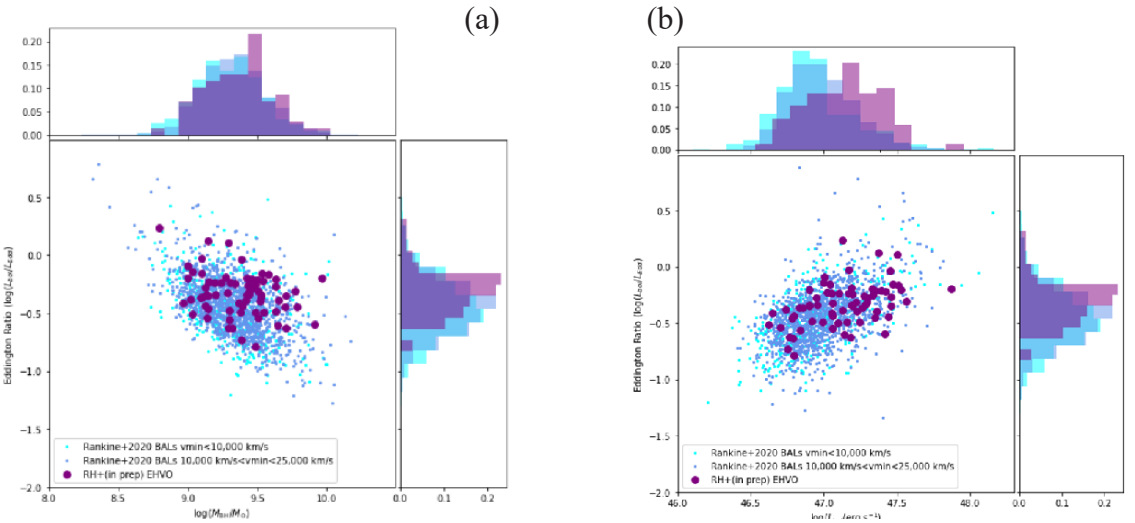

Figure 6. Plots (a) and (b) have the same layout as in Figure 5, but now we plot EHVO quasars and BALQSOs at different speeds. BALs with minimum velocities less than 10,000 km/s appear in light blue, BALs with minimum speeds in between 10,000 km/s and 25,000 km/s in ocean blue, and EHVOs in magenta. The plots show that EHVO quasars have larger bolometric luminosities and Eddington ratios than the BALQSOs at both speeds.

For the histograms we chose the optimal bin size using a method called Knuth's rule (Knuth 2013). This is a method that is based on the data collected, instead of asserting strong prior assumptions about the data, such as assuming the data exhibits a normal distribution. Thus, it is optimal for plotting histograms with complicated data sets. In our case, since we are comparing an uneven number of data points for sets of the parent sample, BALQSOs and EHVOs, we decided to utilize this method to represent the histograms more accurately.

The result of our analysis finds that the black hole mass distribution of the EHVO and parent sample quasars are largely similar. Inspecting Figure 5a (top histogram), where the horizontal axis shows the EHVO and parent sample's M_{bh} distribution, suggests that the shapes of the two histograms are overall matching, meaning there is no significant difference between the two. We see that in Figure 6 (a) the mass distribution histogram (top) for BALQSOs vs EHVOs also does not show significant differences. Given the three groups, quasars with EHVOs, BALs and the parent sample, show similar distributions of black hole mass, we conclude that this is not a parameter that influences the presence or speed of an outflow.

Figures 5b and 6b (top histograms) show that EHVO quasars are the most luminous: both the parent sample's and BALQSO's luminosity distribution trail behind the one that EHVO quasars display. Figure 5b's top histogram represents the parent sample and EHVO's bolometric luminosity distribution. We can see that the distribution of L_{bol} values for EHVO quasars clearly peaks at a larger value than for the parent sample. This conclusion holds true when looking at the top histogram in Figure 6b. Thus, quasars with EHVOs are significantly more luminous than both the parent sample and BALQSOs. The luminosity parameter is therefore likely the reason why these extreme outflows are present in these quasars' spectra.

The distribution of values of Eddington ratios in both figures suggest that the EHVO quasars also show larger values than the other two populations. This is unsurprising because as mentioned previously: L_{bol} correlates with the Eddington ratio. Since values of the bolometric luminosity are larger for EHVOs, while all three quasar groups' black hole mass distributions remain similar, it was expected that EHVOs would also show larger Eddington ratio values. In both Figures 5 and 6, the right histogram shows this relationship clearly, where the peak of the EHVO Eddington ratio is at a significantly larger value than the other two groups. With this information, we find that the quasars with EHVOs accrete mass at a faster rate than both the parent sample and BALQSOs. The Eddington ratio parameter is for the same reason as L_{bol}, influencing the presence of EHVOs.

Summary:

In the first systematic variability study on EHVOs, our preliminary results show that they vary more often than BALQSOs. We observed a large range of variability cases: appearances, disappearances, and large speed changes. Almost half of cases (24/51, 47%) show variability. Of the remaining cases, 20 need the application of further processing techniques to be reclassified, and 7 are confirmed as non-variable.

We find that quasars with EHVO are a distinct class by themselves when compared to BALQSOs and the parent sample of quasars. Two out of three quasar physical parameters are shown to be impactful on the presence of these extreme outflows: EHVOs show larger values of L_{bol} and Eddington ratio relative to the other studied populations, while the M_{bh} parameter does not seem to have any influence on the presence of EHVOs.

Acknowledgements:

All authors would like to thank the NSF-AAG grant award #2107960. E.R.P and V.P would like to thank the Washington NASA Space

Grant Consortium, funded by the NASA office of STEM Engagement, NASA Award 80NSSC20M0104. Additionally, E.R.P would like to thank the Physical Science Division for the summer chair award in research, as well as his parents.

Funding for the Sloan Digital Sky Survey IV has been provided by the Alfred P. Sloan Foundation, the U.S. Department of Energy Office of Science, and the Participating Institutions. SDSS acknowledges support and resources from the Center for High-Performance Computing at the University of Utah. The SDSS web site is www.sdss4.org.

SDSS is managed by the Astrophysical Research Consortium for the Participating Institutions of the SDSS Collaboration including the Brazilian Participation Group, the Carnegie Institution for Science, Carnegie Mellon University, Center for Astrophysics | Harvard & Smithsonian (CfA), the Chilean Participation Group, the French Participation Group, Instituto de Astrofísica de Canarias, The Johns Hopkins University, Kavli Institute for the Physics and Mathematics of the Universe (IPMU) / University of Tokyo, the Korean Participation Group, Lawrence Berkeley National Laboratory, Leibniz Institut für Astrophysik Potsdam (AIP), Max-Planck-Institut für Astronomie (MPIA Heidelberg), Max-Planck-Institut für Astrophysik (MPA Garching), Max-Planck-Institut für Extraterrestrische Physik (MPE), National Astronomical Observatories of China, New Mexico State University, New York University, University of Notre Dame, Observatório Nacional / MCTI, The Ohio State University, Pennsylvania State University, Shanghai Astronomical Observatory, United Kingdom Participation Group, Universidad Nacional Autónoma de México, University of Arizona, University of Colorado Boulder, University of Oxford, University of Portsmouth, University of Utah, University of Virginia, University of Washington, University of Wisconsin, Vanderbilt University, and Yale University.

Bibliography

Barlow, T. A., Junkkarinen, V. T., Burbidge, E. M., Weymann, R. J., Morris, S. L., & Korista, K. T. (1992). Broad Absorption-Line Time Variability in the QSO CSO 203. *The Astrophysical Journal*, 397, 81-87. doi:10.1086/171768

Boroson, T. A., Meyers, K. A., Morris, S. L., & Persson, S. E. (1991). The Appearance of a New Redshift System in Markarian 231. *The Astrophysical Journal*, 370. doi:10.1086/185967

Bosman, S. E., Davies, F. B., Becker, G. D., Keating, L. C., Davies, R. L., Zhu, Y., . . . Yang, J. (2022). Hydrogen reionization ends by z = 5.3: Lyman-α optical depth measured by the XQR-30 sample. *Monthly Notices of the Royal Astronomical Society*, 514(1), 55-76. doi:10.1093/mnras/stac1046

Charles, M., Bunger, D., DeFrancesco, C., García Naranjo, W., Kahassai, N., Parker, M., & Saurav Rijal, A. (2022). Improving Algorithm and Modular Programming in the Search of EHVO in SDSS Quasar Spectra. *THE CROW*, 7, 53-65.

Coatman, L., Hewett, P. C., Banerji, M., Richards, G. T., Hennawi, J. F., & Prochaska, J. X. (2017). Correcting C IV-based virial black hole masses. *Monthly Notices of the Royal Astronomical Society*, 465(2), 2120–2142. https://doi.org/10.1093/mnras/stw2797

Di Matteo, T., Springel, V., & Hernquist, L. (2005). Energy input from quasars regulates the growth and activity of black holes and their host galaxies. *Nature*, 433(7026), 604-607. doi:10.1038/nature03335

Dunbar, B. (2007, November 7 *). A New Kind of Black Hole. Retrieved March 1, 2023, from https://www.nasa.gov/vision/universe/starsgalaxies/Black_Hole.html#:~:text=A%20typical%20stellar%2Dclass%20of,to%20billions%20of%20solar%20masses

Emmering, R. T., Blandford, R. D., & Shlosman, I. (1992). Magnetic acceleration of broad emission-line clouds in active galactic nuclei. *The Astrophysical Journal*, 385, 460. doi:10.1086/170955

Filiz Ak, N., Brandt, W. N., Hall, P. B., Schneider, D. P., Anderson, S. F., Hamann, F., . . . York, D. (2013). Broad absorption line variability on multi-year timescales in a large quasar sample. *The Astrophysical Journal*, 777(2), 168. doi:10.1088/0004-637x/777/2/168

Giustini, M., & Proga, D. (2019). A global view of the inner accretion and ejection flow around super massive black holes. *Astronomy & Astrophysics*, 630. https://doi.org/10.1051/0004-6361/201833810

Hamann, F., Barlow, T. A., Beaver, E. A., Burbidge, E. M., Cohen, R. D., Junkkarinen, V., & Lyons, R. (1995). Ne VIII Lambda 774 and time variable associated absorption in the QSO UM 675. *The Astrophysical Journal,* 443, 606-616. doi:10.1086/175552

Hamann, F., & Sabra, B. (2004). The Diverse Nature of Intrinsic Absorbers in AGN (Vol. 311, p. 203). AGN Physics with the Sloan Digital Sky Survey, Proceedings of a conference held in Princeton, NJ, USA, 27-31 July 2003, Edited by Gordon T. Richards and Patrick B. Hall, ASP Conference Series, Volume 311. San Francisco: *Astronomical Society of the Pacific*, 2004.

Knight, R. D. (2017). *Physics for Scientists and Engineers. A Strategic Approach with Modern Physics*. Pearson.

Knuth, K. H. (2013, September 16). Optimal data-based Binning for histograms. arXiv.org. Retrieved March 1, 2023, from https://arxiv.org/abs/physics/0605197v2

Konigl, A., & Kartje, J. F. (1994). Disk-driven hydromagnetic winds as a key ingredient of active galactic nuclei unification schemes. *The Astrophysical Journal*, 434, 446. doi:10.1086/174746

Rankine, A. L., Hewett, P. C., Banerji, M., & Richards, G. T. (2020). Bal and non-bal quasars: Continuum, emission, and absorption properties establish a common parent sample. *Monthly Notices of the Royal Astronomical Society*, 492(3), 4553–4575. https://doi.org/10.1093/mnras/staa130

Rodríguez Hidalgo, P., et al. (in prep)

Rodríguez Hidalgo, P., Hamann, F., & Hall, P. (2010). The extremely high velocity outflow in quasar PG0935+417. *Monthly Notices of the Royal Astronomical Society*, 411(1), 247-259. doi:10.1111/j.1365-2966.2010.17677

Rodríguez Hidalgo, P., Khatri, A. M., Hall, P. B., Haas, S., Quintero, C., Khatu, V., . . . Murray, N. (2020). Survey of extremely high-velocity outflows in Sloan Digital Sky Survey quasars. *The Astrophysical Journal,* 896(2), 151. doi:10.3847/1538-4357/ab9198

Rodríguez Hidalgo, P., & Rankine, A. L. (2022). Connection between emission and absorption outflows through the study of quasars with extremely high velocity outflows. *The Astrophysical Journal Letters*, 939(2). doi:10.3847/2041-8213/ac9628

Rogerson, J. A., Hall, P. B., Rodríguez Hidalgo, P., Pirkola, P., Brandt, W. N., & Filiz Ak, N. (2016). Multi-epoch observations of extremely high-velocity emergent broad absorption. *Monthly Notices of the Royal Astronomical Society*, 457(1), 405-420. doi:10.1093/mnras/stv3010

Ryden, B. (2016). *Intro to Cosmology* (2nd ed.). Cambridge University Press.

Shen, Y., Richards, G. T., Strauss, M. A., Hall, P. B., Schneider, D. P., Snedden, S., Bizyaev, D., Brewington, H., Malanushenko, V., Malanushenko, E., Oravetz, D., Pan, K., & Simmons, A. (2011). A catalog of Quasar Properties from Sloan Digital Sky Survey Data Release 7. *The Astrophysical Journal Supplement Series*, 194(2), 45. https://doi.org/10.1088/0067-0049/194/2/45

Wu, Q., & Shen, Y. (2022). A catalog of Quasar Properties from Sloan Digital Sky Survey Data release 16. *The Astrophysical Journal Supplement Series*, 263(2), 42. https://doi.org/10.3847/1538-4365/ac9ead